Journal for Geometry and Graphics
Volume 26 (2022), No. 2, 185–205

Cylindrical Dual Tiling Origami

Akito Adachi, Tomohiro Tachi, Yasushi Yamaguchi

The University of Tokyo, Tokyo, Japan
adachi.akito.53u@gmail.com, tachi@idea.c.u-tokyo.ac.jp, yama@graco.c.u-tokyo.ac.jp

Abstract. Non-flat folded origami tessellations folded from one sheet can exhibit a high stiffness to weight ratio. Adachi et al. proposed the dual tiling origami, a family of origami tessellations that forms an octet truss structure between two parallel planes. As the parallel planes are completely tiled by the origami surface, it has a potential advantage when applied as a core material in the sandwich panel. In this study, we extended dual tiling origami to create prescribed cylindrical surfaces by varying the sizes of the alternating regions in the patterns. We showed the conditions that these regions are compatible with each other, and thus they can be folded from a single sheet. Based on the geometric condition, we introduce parameters to design the shapes of the folded state and show the solution space provided by the existence condition. We also geometrically characterize dual tiling origami and illustrate some design examples.

Key Words: Origami, tessellation, foldcore, computer aided design, dual tiling origami

MSC 2020: 52B70 (primary), 52C20, 51M15

1 Introduction

Origami tessellation is the folding of a sheet of paper, in which modular folding patterns are repeatedly applied to the surface. Typical artistic origami tessellations are flat folded; in some cases, they are periodic [3, 6], and in other cases, irregular patterns are generated [11]. In engineering applications, tessellations in non-flat-folded states have often been investigated [14, 15, 21].

These non-flat origami tessellations have two main features. First, globally curved surfaces can be fabricated using a single sheet. Some non-flat origami tessellations form globally curved surfaces [15, 21]. Recent studies have approached the inverse problem: designing curvatures of surfaces by adjusting crease patterns [5, 7, 8, 18, 19]. Second, the structures exhibit high stiffness values. Some non-flat origami tessellations have high stiffness owing to their spatial structures. They have been applied to the cores of lightweight sandwich panels [10, 13]. Compared to other sandwich panels, origami cores have advantages in that they are folded

ISSN 1433-8157/$ 2.50

from a sheet and can be applied on any scale. Some studies further have combined these two features. Klett proposed a deformed Miura-Ori foldcore that approximates a curved surface [9]. Curved foldcores are expected to be used for curved panels such as the body of an airplane.

Most studied foldcores, e.g., cores based on Miura-Ori and waterbomb tessellations, are bonded to two sheets, called skin surfaces, along the edges. The narrow bonding area prevents the core and skin from being firmly brazed or welded; therefore, it is a potential weakness of these sandwich core panels [12, 16]. Therefore, tessellation patterns with bonding areas are preferable to solve this problem. For example, Suto et al. proposed extruded Miura-Ori, which has bonding faces parallel to the skin [17]. A cylindrical foldcore designed by Zhou et al. [20] shows a bonding area if the skin surface is on the side of a prism and is not limited to a right circular cylinder. As an extreme case, Adachi et al. [2] proposed a dual tiling origami that completely fills two planes with faces. When dual tiling origami is used as the foldcore, the faces are bonded to the skin surfaces and are expected to have high resistance against separation. Moreover, if a dual tiling origami is fixed in its three-dimensional state, the tessellation forms a spatial structure equivalent to an octet-truss, and thus can be used as a structural panel without skin surfaces. However, owing to the symmetry required to compose dual tiling origami, previous studies have explored only global planar forms.

This study aimed to generalize dual tiling origami to globally curved surfaces. Specifically, we propose a quadrangular grid dual tiling origami that forms cylindrical surfaces with various profile curves. In Section 2, we introduce planar dual tiling origami as a premise. In Section 3, we explain the strategy to extend dual tiling origami to a cylinder. We derived the geometric conditions for such a structure and introduced the design parameters and solution space. In Section 4, we explain the design approach of cylindrical dual tiling origami and special examples based on geometric properties. In Section 5, we explain that dual tiling origami is not rigid foldable according to our observations. Section 6 shows the design and the fabrication process.

2 Dual Tiling Origami

The octet truss is a truss structure that fills space with regular octahedra and regular tetrahedra. One layer of such a space-filling, composed of half-octahedra (square pyramid) and regular tetrahedra is often used for structural purposes. “Octet Truss, opus 652” by Lang [22] is an origami design that forms a layer of octet truss, where the bars in the truss are realized by the folded creases. “Octet Truss” forms a thick surface, each side of which is filled with squares. Each square is the base of a square pyramid that fills the interior, together with folded regular tetrahedra. The dual tiling origami is a generalization of the “Octet Truss,” where the right square pyramids and regular tetrahedra are replaced by general pyramids and tetrahedra [2].

A dual tiling origami is constructed as follows.

1. Provide two skin surfaces (called the top and bottom surfaces) and draw a planar graph on each surface, such that the graphs on both sides are dual. The top (bottom, resp.) pyramids are constructed by connecting the faces on the top (bottom, resp.) graph and the corresponding vertices at the bottom (top, resp.) graph, as indicated in red (gray, resp.) pyramids in Fig. 1. Tetrahedra are constructed by connecting dual edges as shown in the blue region in Fig. 1; they are surrounded by pyramids. The bases of the top and bottom pyramids are the faces of the top and bottom graphs, respectively.

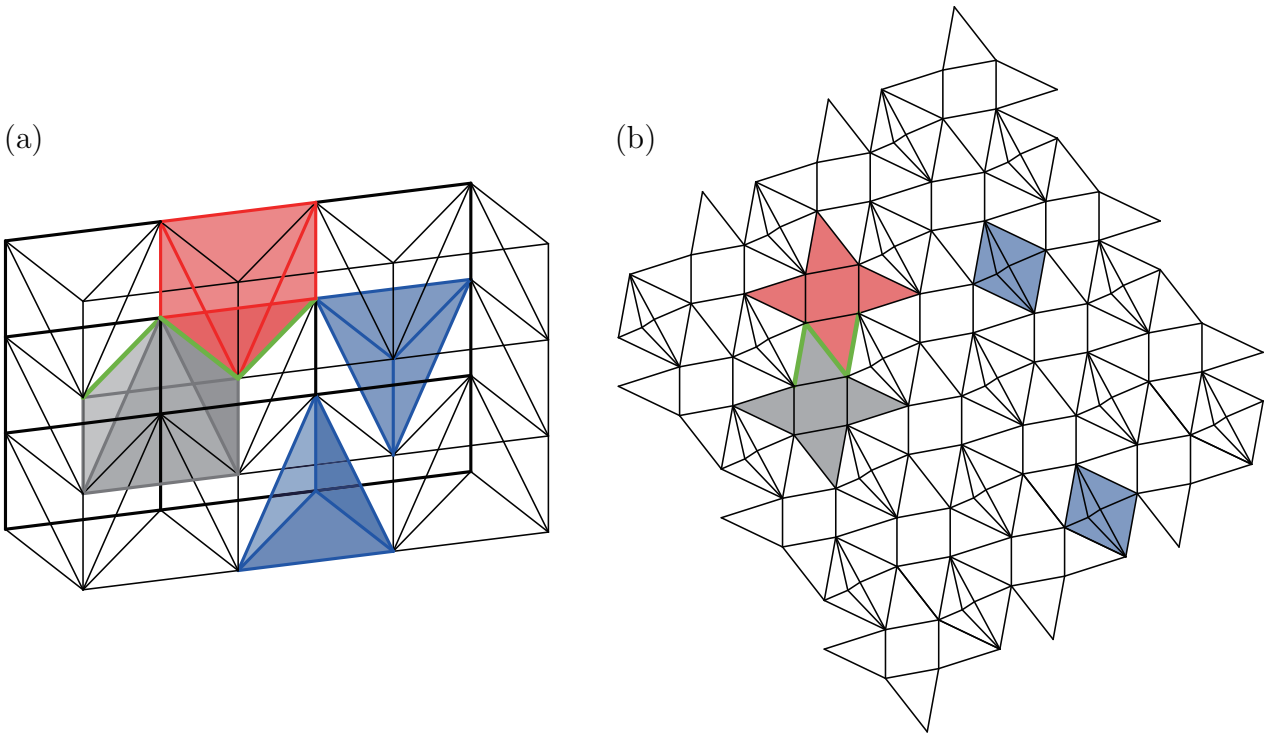

Figure 1: Planar dual tiling origami. (a) Truss structure, (b) Crease pattern. Red and gray pyramids correspond to red and gray petal polygons. Blue tetrahedra correspond to blue quadrangles.

2. Cut the ridgelines and develop pyramids to form star-shaped polygons called *petal polygons* [1], as indicated by the red and gray regions in Fig. 1(b). We refer to these petal polygons as *pyramid regions*. Here, we place the top pyramid regions outside up and bottom pyramid regions inside up. We place the corresponding pyramid regions between two pyramids that share a ridge, gluing the pyramid regions to share one of the corresponding edges. Because a ridge in the pyramid corresponds to two split edges in the development, we choose a consistent side for gluing. Specifically, we allow the edges of triangles incident to the gluing edge in green in Fig. 1 to form a Z-shape in the top view of the crease pattern.
3. If the connected pyramid regions are placed on a plane, the remaining parts of the plane are quadrangles disconnected from each other (blue regions in Fig. 1(b)). Each quadrangle is referred to as a *tetrahedron region*. The four boundary edges of the tetrahedron region were shared with different pyramid regions. These pyramid regions are folded into pyramids surrounding the corresponding tetrahedron. Add a proper crease pattern to each tetrahedron region, allowing them to be folded into these tetrahedra.

The necessary and sufficient conditions for constructing a dual tiling origami from given skin surfaces and dual graphs are as follows [2]:

Non-intersect condition: Pyramids constructed from dual graphs have no intersection.
Pyramid condition: Pyramid regions are placed on a plane without gaps or overlaps.
Tetrahedron condition: Valid creases are added to each tetrahedron region as they are folded into the corresponding tetrahedron.

In this study, we considered a subset of dual tiling origami, whose graphs are grids of parallelograms with degree-4 vertices.

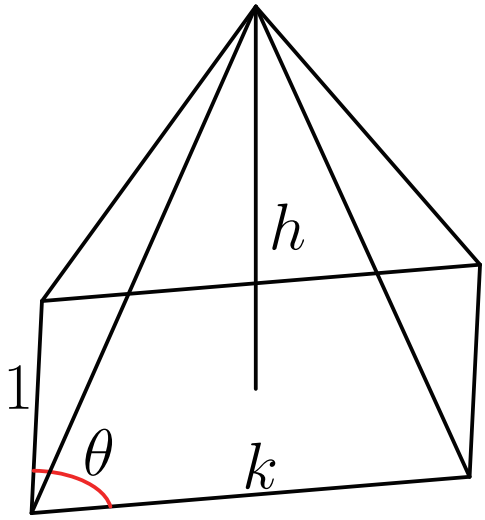

Figure 2: Parameters that represent a two-fold symmetric pyramid.

2.1 Planar Parallelogram Dual Tiling Origami

In this section, we present a type of globally planar parallelogram dual tiling origami with two-fold symmetric pyramids. Their skin surfaces are parallel planes. Dual graphs are congruent parallelogram lattices. The relative positions of the graphs are such that perpendiculars from the vertices of a graph pass through the center of the faces of another graph. The dual graphs then create a truss structure whose pyramids are right and congruent, as shown in Fig. 1. The result from [2] is as follows:

Non-intersect condition: The non-intersect condition is always satisfied because the pyramid is a right pyramid.

Pyramid condition: Because the pyramid regions are two-fold symmetric, there exist two parallel translations that tile the pyramid regions without gaps. This guarantees the pyramid condition, except when the pyramid regions overlap. Overlapping occurs when the sum of the inner angles around a vertex is greater than 2π for certain types of pyramid regions.

Tetrahedron condition: The tetrahedron condition is satisfied if and only if there is a folding of each tetrahedron region that (1) fits the edges of the tetrahedron region (in 2D) into the corresponding edges of the corresponding tetrahedron (in 3D) and (2) folds the rest of the paper inside the tetrahedron. According to Demaine and Ku [4], condition (1) is equivalent to each diagonal edge in 2D being longer than or equal to the distance between the corresponding opposite vertices in 3D, which is the edge length of the base of a pyramid in parallelogram dual tiling origami. If a quadrangle is convex and satisfies condition (1), the crease patterns shown in Fig. 1 fold the rest of this paper to satisfy condition (2). As the tetrahedron regions in the planar parallelogram dual tiling origami are convex, condition (1) is sufficient for the tetrahedron condition.

We state that the tetrahedron condition is *critically satisfied* when one of the lengths of the diagonal edge is equal to the distance between corresponding opposite vertices in the folded state. In this case, the crease pattern in the tetrahedron region became a single crease along the diagonal edge. We call this tetrahedron region *critical*. Critical tetrahedron regions are often preferable, because they can be folded from a pattern with a small number of creases.

The planar parallelogram dual tiling origami can be parameterized by three parameters

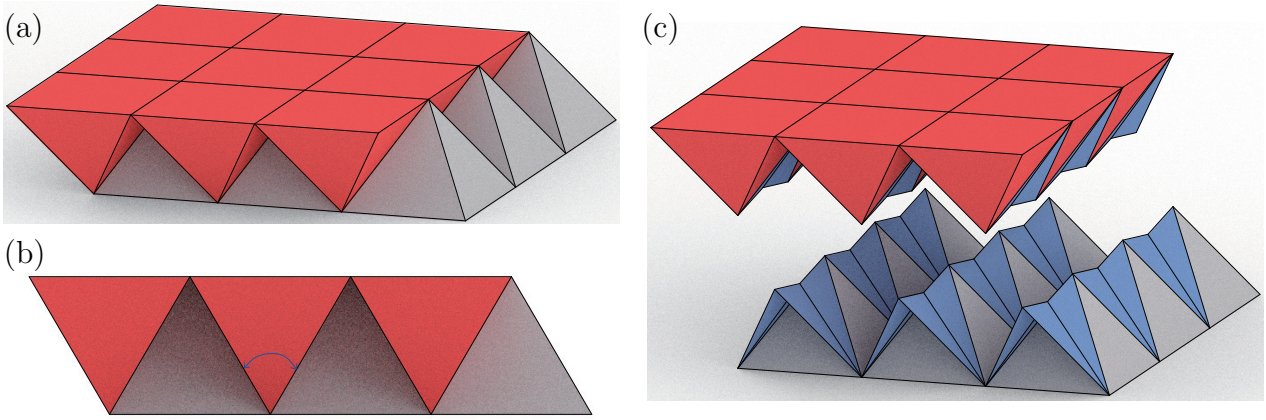

Figure 3: Division to wedges shown in Fig. 4. (a) Planar parallelogram dual tiling origami without tetrahedron regions, (b) Projection of (a) along an edge on the skin surface, (c) The same sets of wedges whose bases are top and bottom surfaces combine to make a planar dual tiling origami.

up to similarity: one of the edge lengths k, parallelogram angle θ, and the height h, as shown in Fig. 2. Then, the tetrahedron condition is expressed as follows:

$$\left((k-\cos\theta)\sin\theta-\cos\theta\sqrt{4h^2+\sin^2\theta}-\sqrt{4h^2+k^2\sin^2\theta}\right)^2 + \left(\sin^2\theta+2k\cos\theta+\sin\theta\sqrt{4h^2+\sin^2\theta}\right)^2 \geq 4k^2, \tag{1}$$

$$\left((k-\cos\theta)\sin\theta-\cos\theta\sqrt{4h^2+\sin^2\theta}+\sqrt{4h^2+k^2\sin^2\theta}\right)^2 + \left(1+\cos^2\theta-\sin\theta\sqrt{4h^2+\sin^2\theta}\right)^2 \geq 4. \tag{2}$$

When the pyramids satisfy these inequalities, the sum of the inner angles of the pyramid regions around a vertex is smaller than 2π; thus, so the pyramid condition is also satisfied. That is, the necessary and sufficient condition to complete a planar parallelogram dual tiling origami with congruent two-fold symmetric pyramids is to satisfy inequalities (1) and (2).

3 Cylindrical Parallelogram Dual Tiling Origami

3.1 Unit Wedge

We consider the decomposition of planar parallelogram dual tiling origami into wedges. From the truss structure of a planar parallelogram dual tiling origami in Fig. 3 (a), there is a row of pyramids along the base edge and tetrahedra between them. We refer to this structure as a wedge (Fig. 4). The bases of the pyramids formed the *base* of the wedge. The edge on the other side of the base is called the *apex edge*, and is represented by a green segment. The trapezoidal faces incident to the apex edge are called *trapezoid sides*. The angle between the trapezoid sides is called the *wedge angle* (Fig. 4 (a)). Combining the translated and rotated copies of the wedges alternately constitutes the original truss structure (Fig. 3 (c)).

To generalize parallelogram dual tiling origami into curved origami, we consider combining multiple types of wedges. The skin surfaces are bent by having wedges of different wedge angles from the top and bottom sides. Because the skin surface is bent in the direction of

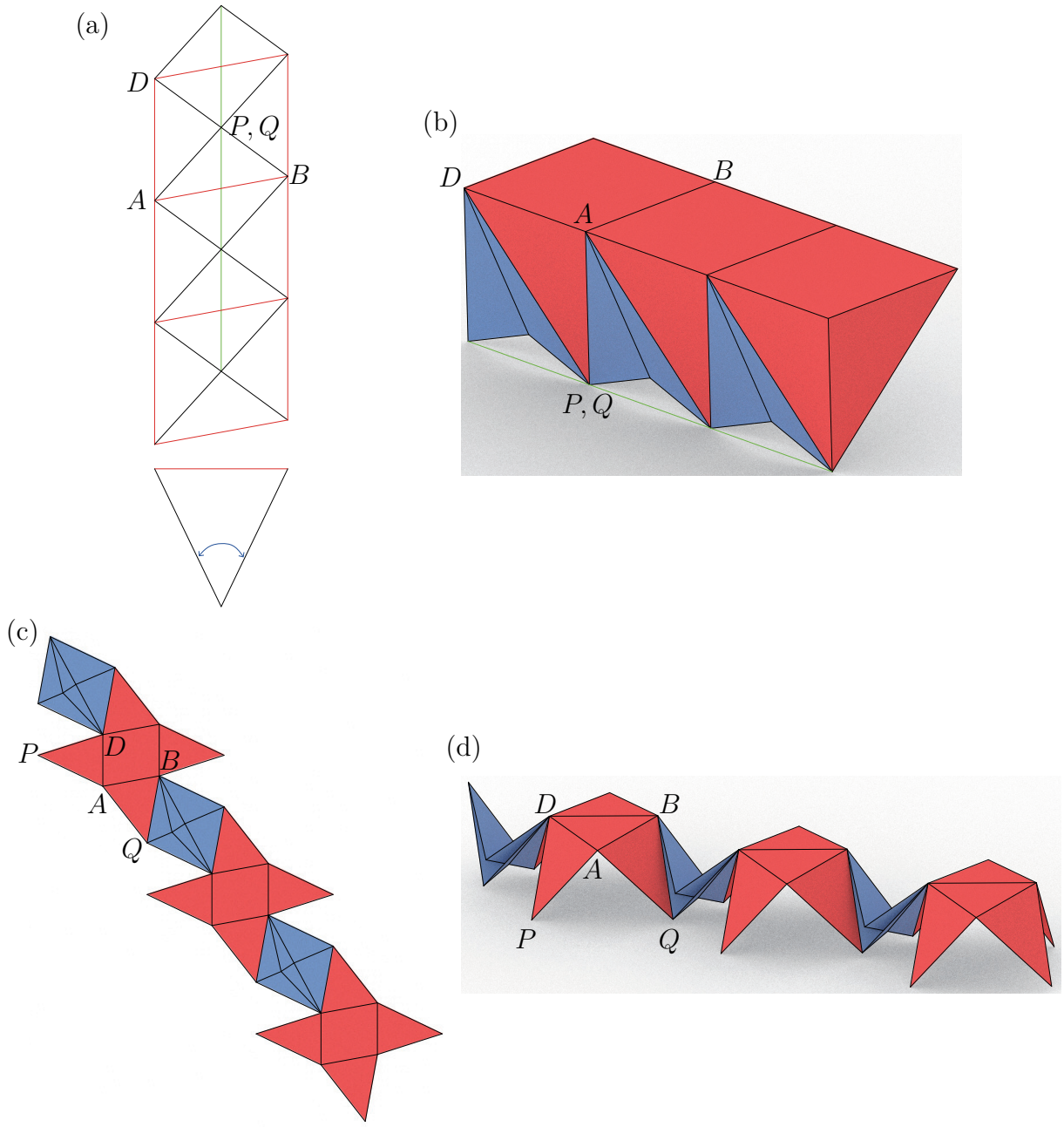

Figure 4: Unit wedge. Alphabets represent vertices corresponding to Fig. 6. (a) Top and front views of truss belong to a unit wedge, (b) Folded state of a unit wedge. Base: the union of the base of the red pyramid, Apex edge: the green line, Trapezoid side: the face of the convex hull of the unit wedge on which the apex edge is located. Wedge angle: the dihedral angle of the trapezoid sides, represented by blue arrows in (a), (c) Developed state of a unit wedge, (d) Intermediate state of folding a unit wedge. The diagonal of the bottom face of each pyramid is folded, and some creases in tetrahedron regions are moving during the folding motion (See Section 5).

apex edges, the resulting surface is a generalized cylinder whose ruling lines are parallel to the apex edges. We refer to such parallelogram dual tiling origami with multiple types of wedge as *cylindrical parallelogram dual tiling origami*. The next Section explains the conditions for combining multiple types of wedges. Here, we assume that the pyramids in each wedge are congruent and two-fold symmetric.

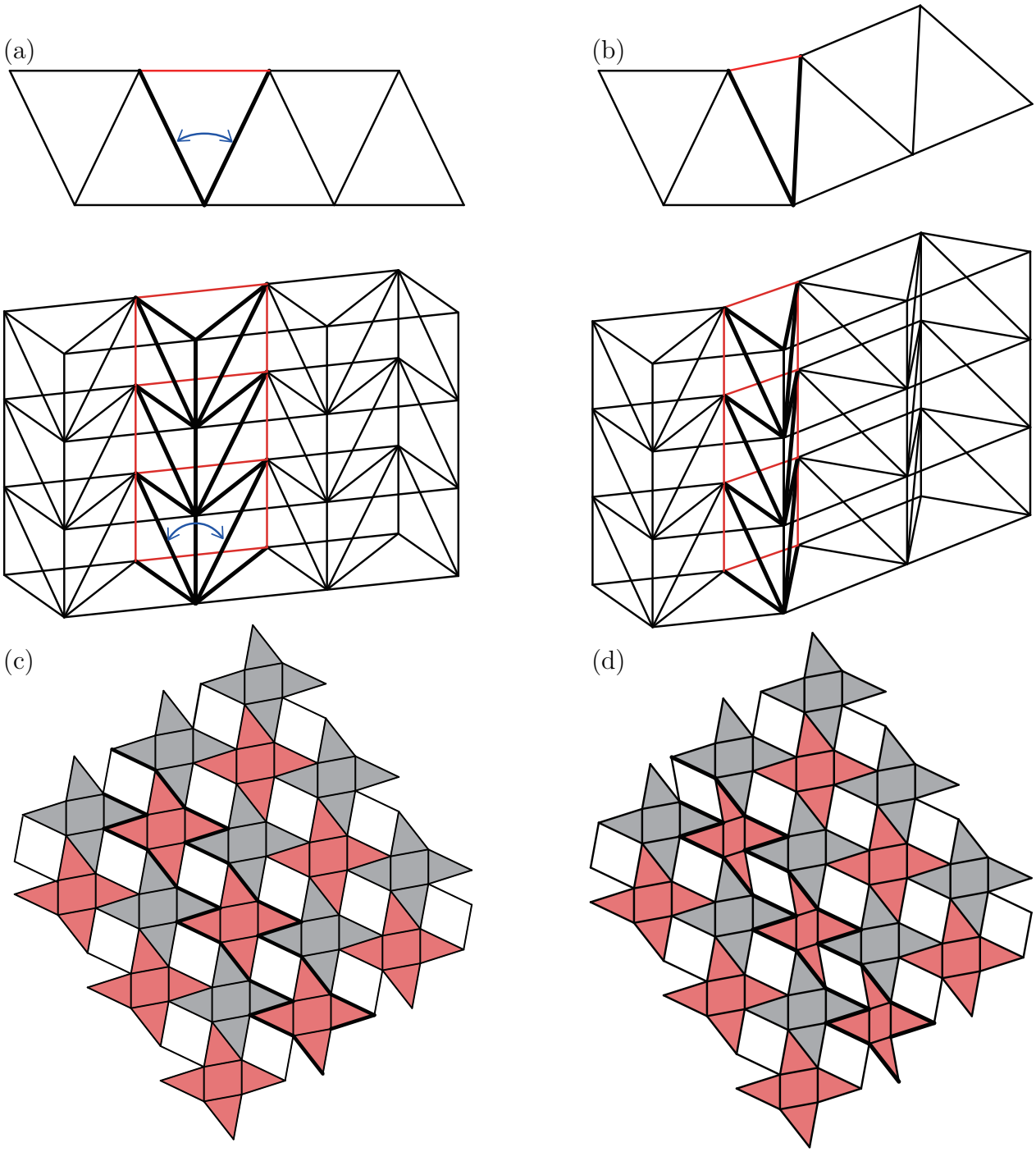

Figure 5: Replacement of a wedge in a planar parallelogram dual tiling origami. (a) Original truss structure, (b) Deformed truss structure, (c) Developed state of the original parallelogram dual tiling origami, (d) Deformed developed state.

3.2 Compatibility of Wedges

We now consider the compatibility between different wedges (refer to Fig. 5). We consider replacing the wedge of a planar parallelogram dual tiling origami with a different one. This changes the truss structure from (a) to (b). The trapezoid sides of the replaced wedge are congruent with those of the original wedge. Therefore, the replaced wedge was obtained from the original wedge by rotating one trapezoid side around the apex edge. With this rotation,

the base of the wedge stretches (or shrinks) in the direction perpendicular to AD in Fig. 4, which is parallel to the apex edge.

Then, we observe the changes in the developed state from (c) to (d) in Fig. 5. We consider the deformation of the developed wedge between two bold polylines. Because the wedges adjacent to the deforming wedge do not deform, the bold polylines can only transform, and the shapes cannot deform. Figure 6 shows the close-up view of a part of Fig. 5 (c) and (d). The deformation of the wedge does not change the position of the vertices A, D, P, and Q. From the aforementioned observation of the truss, the base of the pyramid is stretched (or shrunk) perpendicular to edge AD. In other words, the deformed vertex B' must be on the blue perpendicular from vertex B to edge AD during development. Because the ridges of pyramids do not deform, split ridges $B'Q, BQ$ must also have the same length. Therefore, vertex B' must be on the blue circle that passes through vertex B and has the vertex Q as its center. In Summary, vertex B' is drawn as the intersection of the blue line and blue circle. From fixed vertices A, B', D, P, Q, we can draw the entire pyramid region using two-fold symmetry.

When the original pyramids in Fig. 6 are fixed, at most one vertex B' that differs from B is constructed. By contrast, from the pyramid region with the vertex B', the vertex B can be constructed in the same way. In other words, only a pair of pyramids corresponding to B and B' is compatible. The pair completes the potential types of components in cylindrical parallelogram dual tiling origami. When BQ and AD are parallel, the constructed point B' coincides with B. In this case, we obtain only a single type of wedge, and thus we can only form a planar parallelogram dual tiling origami.

3.3 Necessary conditions of Derived Pyramid

It has not yet been proven that the constructed pyramid region is the developed state of a pyramid. First, we check the non-intersection of the constructed pyramid region. In Fig. 6, we consider an orthogonal coordinate system where the origin is vertex A and the y axis is the vector $\overrightarrow{AD}$. Vertex B' should be located on the right side of AD, otherwise, base parallelogram flips (see the failure case in Fig. 7 (a)), that is, $B'_x > 0 = A_x$. Because $Q_x = (B_x + B'_x)/2$, Q_x should be closer to B_x than it should be to A_x. The condition is equivalent to

$$0 < \angle DAB < \frac{\pi}{2}. \tag{3}$$

We note that in the case $\angle DAB = \pi/2$, the derived pyramid is degenerate, that is, $B' = A$. Degenerate cases are discussed in Section 4.3.

Another invalid case is illustrated in Fig. 7 (b). In this case, the heights of the sides ADP and $B'AQ$ are insufficient to gather corners to a single apex and form the pyramid. To avoid this, the original pyramid region must satisfy

$$B_x \geq 2Q_x + 2P_x. \tag{4}$$

We note that if the original pyramid region satisfies the tetrahedron condition of a planar parallelogram dual tiling origami, it also satisfies inequality (4).

Inequalities (3) and (4) are the only necessary conditions, and the derivation of the sufficient condition requires a complex case analysis. Instead of using the current parameterization based on one of the pyramids, in the next section, we provide new design parameters that handle both pyramid shapes and describe the necessary and sufficient conditions using these parameters.

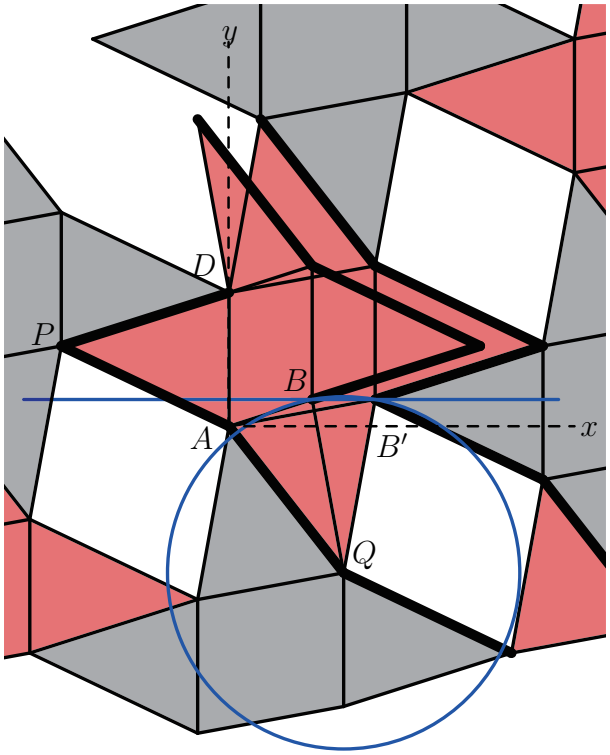

Figure 6: Construction of the counterpart of the pyramid regions that can be connected in the truss structure and the developed state. The vertex B' is defined from the perpendicular from B to AD and the circle whose center is Q and radius is the length of QB. An orthogonal coordinate system is introduced, where the origin is the vertex A and the y axis is parallel to the edge AD.

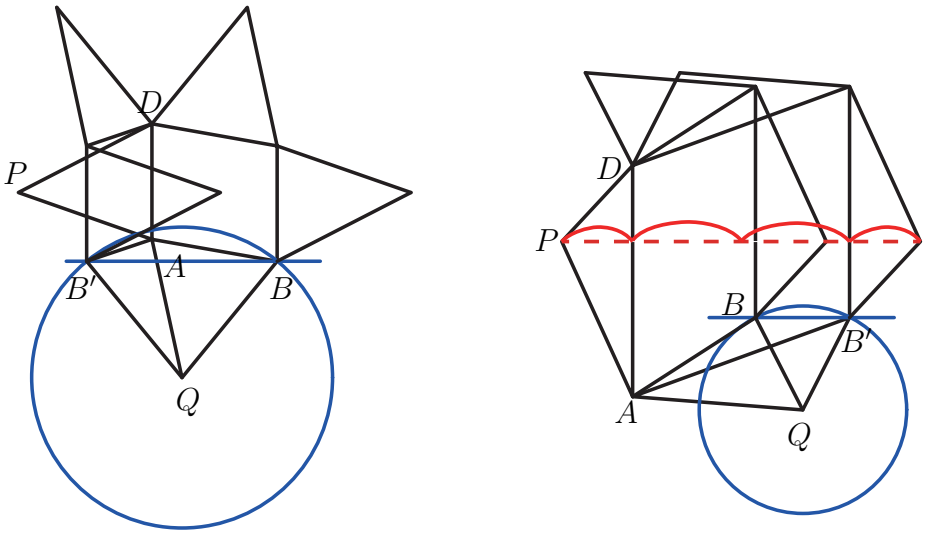

Figure 7: Invalid cases. (a) The base parallelogram flips, (b) Side heights are insufficient to form a pyramid.

3.4 Design Parameters

The number of parameters to describe the pair of wedges is three because one of the pairs of wedges parameterized by k, θ, and h uniquely determines the other wedge, as shown in Section 3.2. Here, we assume that the length of edge DA in Fig. 6 is one.

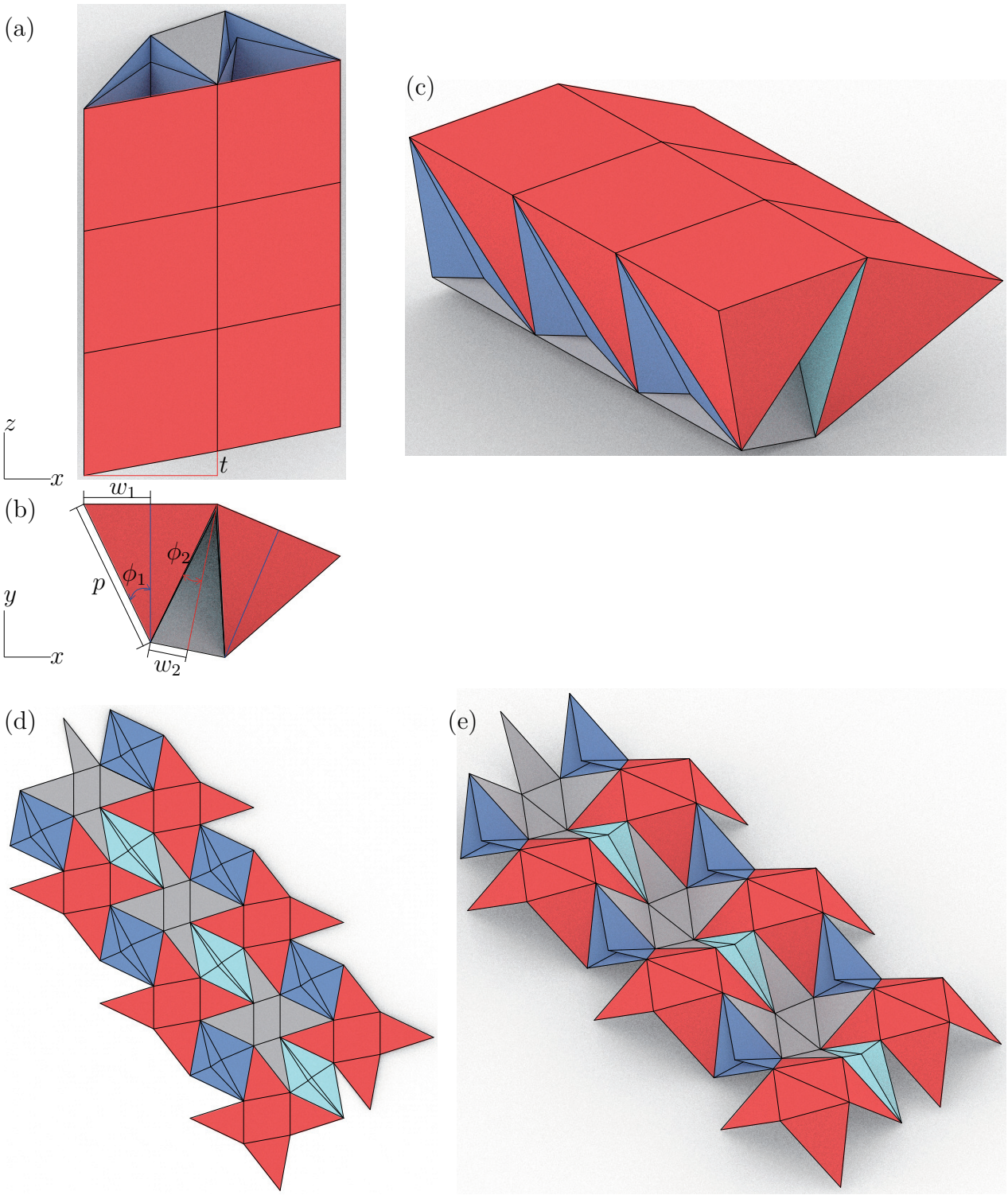

Figure 8: Parameters to design a cylindrical parallelogram dual tiling origami. p: oblique side of a projected wedge along the apex edge, w_i: half of the bottom side of the projected wedge, h_i: height of the projected wedge, ϕ_i: half of the wedge angle. (a) Top view perpendicular to the base of the leftmost wedge, (b) Front view parallel to the apex edges, (c) Perspective view, (d) Developed state, (e) Intermediate state of folding.

We introduce new parameters ϕ_1, ϕ_2, and t suited for designing a folded state of a cylindrical parallelogram dual tiling origami (see Fig. 8). The first two parameters ϕ_1, $\phi_2 \in (0, \pi/2)$

are half of the wedge angles of the two wedges (wedges 1 and 2, respectively) projected along the apex edges (Fig. 8 (b)). These parameters are key factors for creating a curvature. When wedges 1 and 2 are joined, the normal directions (measured along the front side of the sheet of paper) of the bases of the wedges form an angle difference $\phi_1 - \phi_2$, called the *curve angle*. This bending by the curve angle occurred at each contact between the different wedges. For example, in Fig. 8, the bending of the skin surface is produced by joining wedges 1, 2, and 1 in this order; the bending angle is twice the curve angle $2(\phi_1 - \phi_2)$.

The last parameter $t > 0$ is the *shift distance* (Fig. 8 (a)), which is the amount of shift of the parallelogram base, shown by $k\cos\theta$ in Fig. 2. The domain of t is expressed by the necessary condition (3) of the existence of a non degenerate wedge pair. According to the compatibility explained in Section 3.2, the shift distance is common for both types of wedges and accepts a positive value. When concatenating wedges to form a skin surface, the base pyramids shift along the apex edge direction by the shift distance each time a wedge is added to the skin surface.

We can construct the shapes of the wedges after obtaining the length p of the oblique sides of the isosceles triangles in the projection of the wedges (Fig. 8 (b)). Here, we show that p is uniquely determined by three parameters, ϕ_1, ϕ_2, and t because of the compatibility condition. We prepared the other derived parameters as follows: the widths of bases $2w_1$, $2w_2$ and the heights of wedges h_1, h_2 are

$$w_1 = p\sin\phi_1,\ w_2 = p\sin\phi_2, \tag{5}$$
$$h_1 = p\cos\phi_1,\ h_2 = p\cos\phi_2. \tag{6}$$

We can draw the development of pyramids using p, t, ϕ_1, and ϕ_2 in the coordinate system shown in Fig. 6. Wedges 1 and 2 share the same vertices D, P, A and have different vertices B and B' sharing the same y coordinate t as

$$A\begin{pmatrix}0\\0\end{pmatrix},\ B\begin{pmatrix}2w_1\\t\end{pmatrix},\ B'\begin{pmatrix}2w_2\\t\end{pmatrix},\ D\begin{pmatrix}0\\1\end{pmatrix},\ P\begin{pmatrix}-p\\\frac{1+t}{2}\end{pmatrix}. \tag{7}$$

The positions Q and Q' of wedges 1 and 2 are provided to satisfy $|AQ| = |AP| \wedge |BQ| = |PD|$ and $|AQ'| = |AP| \wedge |B'Q'| = |PD|$, respectively. Q and Q' do not coincide for arbitrary p, resulting in a violation of the pyramid condition. By applying the pyramid condition $Q = Q'$, $|BQ| = |B'Q|$ locates Q on the perpendicular bisector of the segment BB'. We can set the coordinates of Q,

$$Q\begin{pmatrix}w_1 + w_2\\q\end{pmatrix}, \tag{8}$$

where by simultaneously solving $|AQ| = |AP|$ and $|BQ| = |PD|$ assuming $t > 0$, we obtain

$$p = \frac{t}{2\sin\phi_1\sin\phi_2}\sqrt{1 + \frac{2}{t}\sin\phi_1\sin\phi_2 - \sin^2\phi_1 - \sin^2\phi_2}, \tag{9}$$
$$q = \frac{1+t}{2} - \frac{2w_1w_2}{t}. \tag{10}$$

3.5 Solution Space

We explain the existence condition with the parameters ϕ_1, ϕ_2, and t by checking the non-intersect, pyramid, and tetrahedron conditions. The non-intersect condition was always satisfied. The pyramid condition states that the development of the pyramids tessellates the

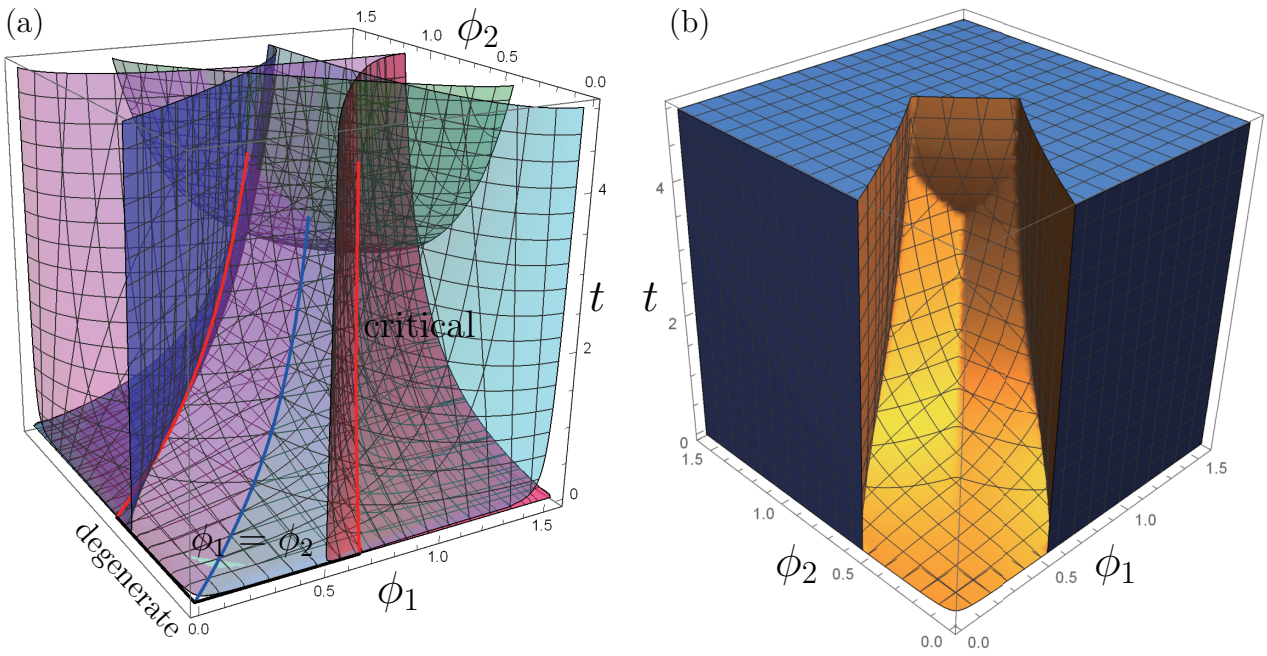

Figure 9: (a) Boundary of the conditions for the design parameters. Red and magenta: the tetrahedron conditions for wedge 1, blue and cyan: the tetrahedron conditions for wedge 2, green: the existence of p. Parameters on the blue curve make wedges congruent and tetrahedron conditions critical. Parameters on the red curves make tetrahedron conditions critical. One of the pairs of wedges degenerates with parameters on the black lines. (b) Solution space for the design parameters. Parameters in the blank area, construct a parallelogram dual tiling origami.

plane and do not overlap. Tessellation is guaranteed if $Q = Q'$, which is satisfied if solutions (9) and (10) are real values. This is equivalent to

$$(-1 + \sin^2\phi_1 + \sin^2\phi_2)\, t \leq 2 \sin\phi_1 \sin\phi_2. \tag{11}$$

The condition that the pyramid regions do not overlap is implied by the tetrahedron condition for the same reason as in the case of planar parallelogram dual tiling origami. Therefore, we checked the tetrahedron condition.

Here, we consider the tetrahedron condition. A parallelogram dual tiling origami with two types of wedges has two corresponding types of tetrahedra and thus two types of tetrahedron regions, as shown in Fig. 5 (d). We note that the tetrahedron condition for each tetrahedron is local to the wedge containing the tetrahedron. This means that the tetrahedron condition for a cylindrical parallelogram dual tiling origami with wedges types 1 and 2 is equivalent to satisfying the tetrahedron conditions for the planar parallelogram dual tiling origami using only wedge 1 and the planar parallelogram dual tiling origami using only wedge 2. They are expressed by

$$\begin{aligned}(p - \sigma_i(w_1 - w_2))^2 + \left(t + \frac{2w_1w_2}{t}\right)^2 \\ \geq ((w_1 + w_2) + \sigma_i(w_1 - w_2))^2 + t^2,\end{aligned} \tag{12}$$

$$(-p - \sigma_i(w_1 - w_2))^2 + \left(1 - \frac{2w_1w_2}{t}\right)^2 \geq 1, \tag{13}$$

where $\sigma_1 = 1$ and $\sigma_2 = -1$ represent the conditions for tetrahedron regions 1 and 2, respectively.

By combining all conditions, parameters ϕ_1, ϕ_2, t ($\phi_1, \phi_2 \in (0, \frac{\pi}{2})$, $t > 0$) satisfy the inequalities (11), (12) and (13) are the necessary and sufficient conditions to construct a cylindrical parallelogram dual tiling origami. The solution space that satisfies the inequalities is shown in Fig. 9. Equations (12) and (13) for $i = 1$ have equality on the red and magenta surfaces, respectively, in Fig. 9 (a). Equations (12) and (13) for $i = 2$ are equal on the blue and cyan surfaces, respectively. The region below the green surface satisfies $p \in \mathbb{R}$, that is, inequality (11). The intersection of these inequalities, indicating the valid parameters for a parallelogram dual tiling origami, is shown as the blank region in Fig. 9 (b).

There are three sets of parameter values where the two tetrahedron regions are critical. The blue curve, that is, the intersection of the magenta and cyan surfaces, satisfies $\phi_1 = \phi_2$. In this case, the pair of pyramids is congruent, and the dual tiling origami becomes planar. The other two sets, where two tetrahedron conditions are critically satisfied, are on the red curves, the intersection of the red and cyan, or the blue and magenta surfaces. By symmetry, we can assume that $\phi_1 > \phi_2$ and consider the intersection of the red and cyan surfaces without loss of generality. By performing the intersection of the equalities in (12) for $i = 1$ and (13) for $i = 2$, we obtain the condition for the red curve as follows:

$$\sin\phi_2 = -1 + \sin\phi_1 + \sin^2\phi_1, \tag{14}$$

$$t = \frac{\sin\phi_2}{\sin\phi_1 - \sin\phi_2}. \tag{15}$$

Previously, we assumed that $t > 0$. We can consider the limit $t \to 0$ when $\min\{\phi_1, \phi_2\} \to 0$ and $\angle DAB = \pi/2$ to provide a degenerate pattern, where one of the bases degenerates to a line segment, as discussed in Section 4.3.

On the green surface in Fig. 9 (a), when t approaches the right-hand side of (11), $p = w_1 = w_2 = h_1 = h_2 = 0$, and all the creases degenerate to a line segment; therefore, this limit cannot be used as an origami pattern.

4 Design and Special Examples

We implemented an interactive design system for parallelogram dual tiling origami using *grasshopper* on *Rhinoceros*. The system computes the folded shape and crease pattern of a parallelogram dual tiling origami from parameters ϕ_1, ϕ_2, and t; therefore, we can edit the parameters interactively while observing the truss structure in 3D and the crease pattern. For the given parameters ϕ_1, ϕ_2, and t, the system also checks that the tetrahedron conditions (12) and (13) are satisfied.

In addition, the system solves the following inverse problems:

1. finding ϕ_1 and ϕ_2 from given $\phi_1 - \phi_2 > 0$ and t, such that they critically satisfy one of the tetrahedron conditions (cyan or red in Fig. 9) through Newton's method.
2. finding ϕ_2 and t from ϕ_1 such that they critically satisfy two tetrahedron conditions by solving equations (14) and (15).

Given a pair of wedges, 1 and 2, we can concatenate them in any order. We present the sequence of types of wedges in the design system to produce cylindrical surfaces with different profiles. For example, if two types of edges appear alternately, that is, "1212 . . . ", we obtain a roughly circular cylindrical surface, as shown in Fig. 11. Figure 12 shows the use of pattern "111222 . . . " to reduce the curvature of the cylinder. Figure 10 shows skin surfaces, such as a sine curve using the sequence "112221212122211 . . . ". The cylindrical form can be represented

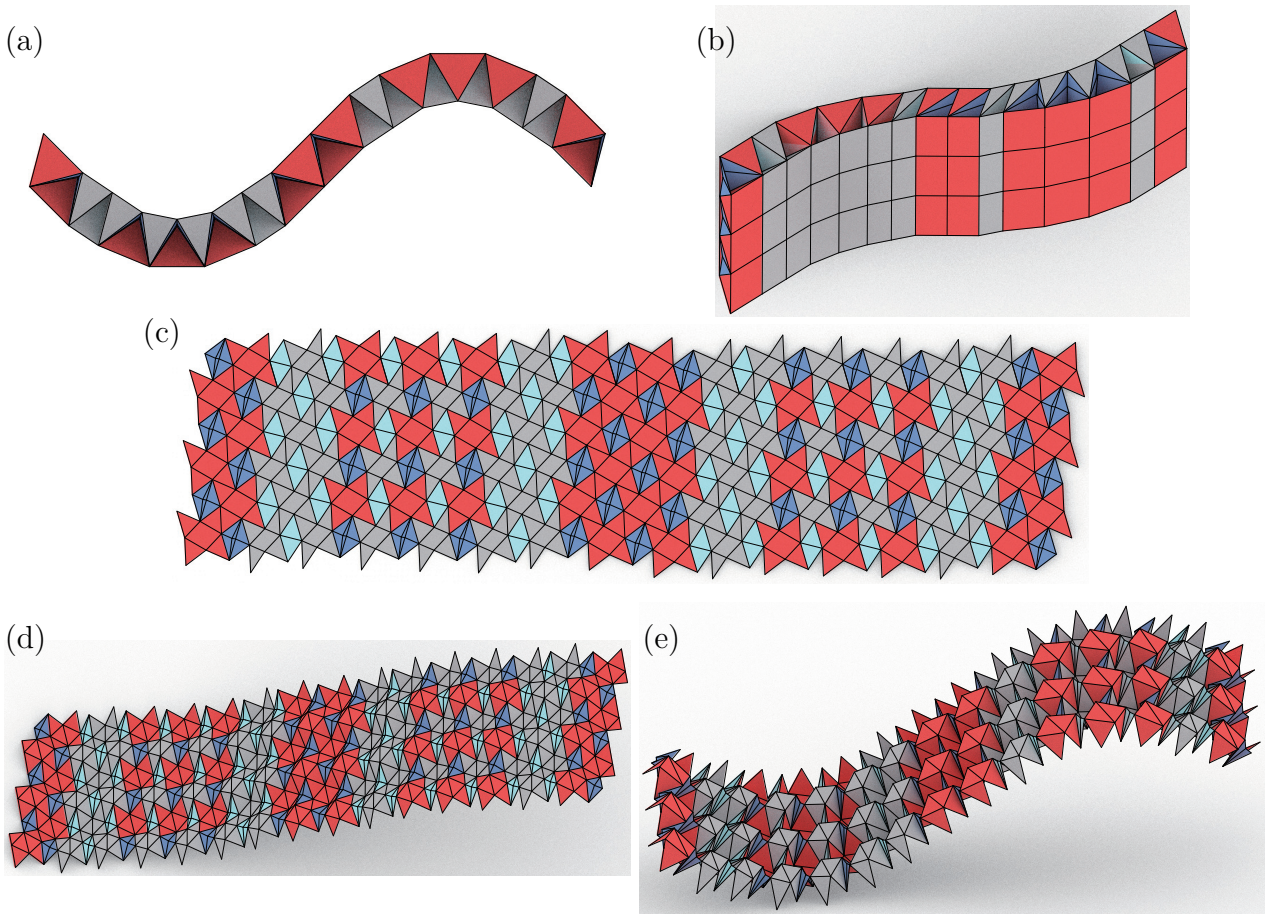

Figure 10: Cylindrical parallelogram dual tiling origami similar to a sine curve, where $\phi_1 \simeq 0.528429, \phi_2 \simeq 0.332079$, and $t = 1/4$. (a) Projection along the apex edges, (b) Oblique view, (c) Crease pattern, (d)(e) Intermediate states of folding.

by a polyline, where the length of each segment is expressed as an integer multiple of $2w_1$ or $2w_2$, and the angle at the corner is expressed by $\pm(\phi_1 - \phi_2)$. Although the angle is not controllable, the overall curvature can be controlled by the segment lengths. In theory, any profile curve can be approximated using $\phi_1 \simeq \phi_2$ with small w_1 and w_2; however, this requires many wedges.

In the following subsections, we introduce design examples with special properties.

4.1 Gently Curved Skin Surfaces

When $\phi_1 = \phi_2$, the two wedges are congruent, and the dual tiling origami becomes planar. When the circle and horizontal lines are tangent, $\phi_1 = \phi_2$ is equivalent to $BQ \parallel DA$, as shown in Fig. 6. Notably, that these parallelogram dual tiling origami are a special subset of planar parallelogram dual tiling origami with congruent pyramids.

As shown in Fig. 9, we can choose the parameters in the neighborhood of the plane $\phi_1 = \phi_2$. Cylindrical parallelogram dual tiling origami with a small curve angle exists. In Fig. 11, one wedge resembles the other, and the tetrahedron condition for a wedge is critically satisfied. The curve angle is $|\phi_1 - \phi_2| = \pi/72$. The sides of a 72-gonal prism are formed by 144 wedges lined up alternately. As shown in Fig. 11 (a), each tetrahedron region protrudes from its tetrahedral room. However, pushing the bulge creates a dent, and we can fold the

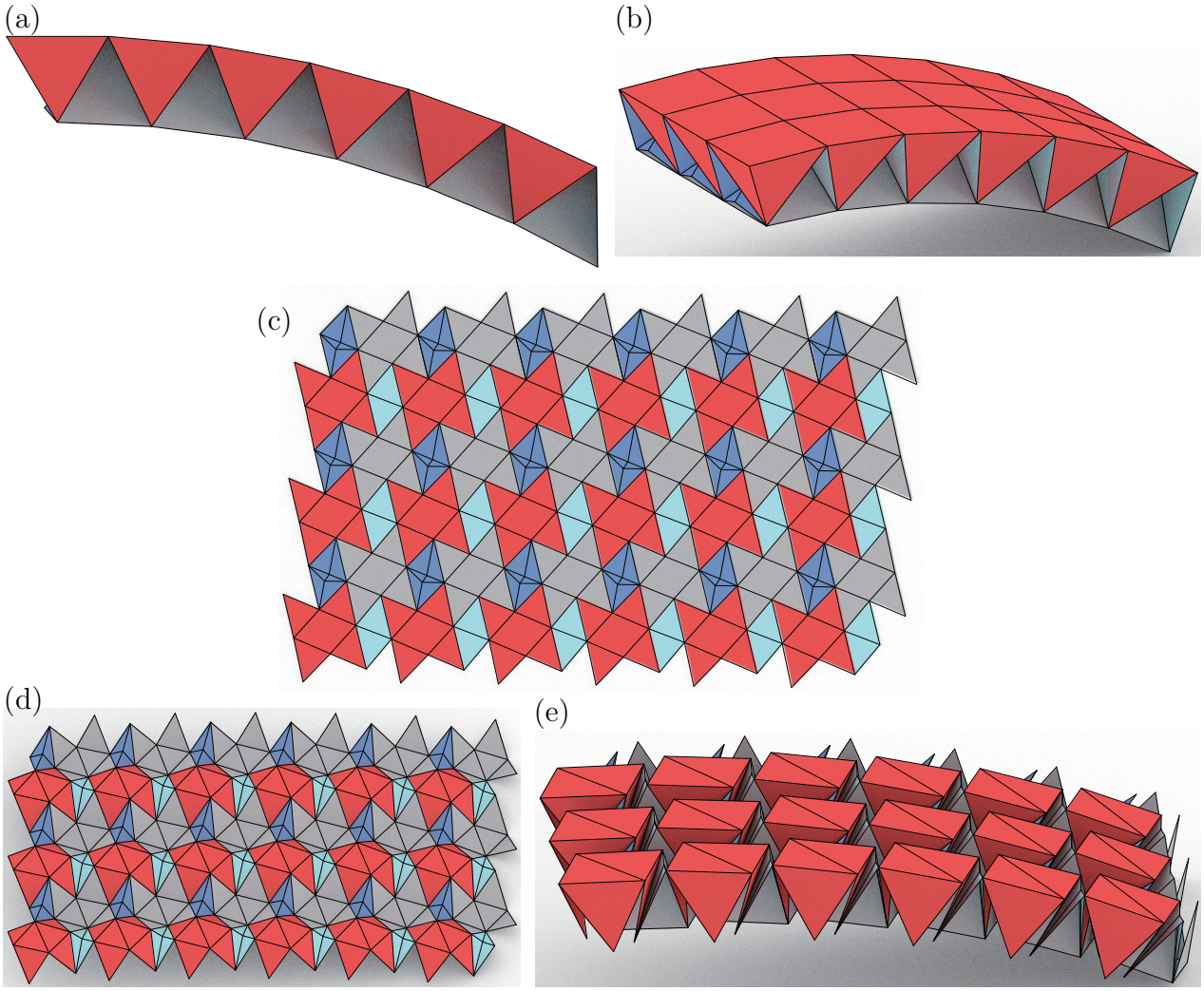

Figure 11: Cylindrical parallelogram dual tiling origami that forms one round with 144 wedges, where $\phi_1 \simeq 0.534928, \phi_2 \simeq 0.491295$, and $t = 1/3$. (a) Projection along the apex edges, (b) Oblique view, (c) Crease pattern of four wedges surrounded by the green frame in (a), (d)(e) Intermediate state of folding.

region into its room.

4.2 Tubular Parallelogram Dual Tiling Origami

When the curve angle is represented by π/n with an integer n, and the shift distance is a rational number, the wedges can form a closed tube. With integers n, f, g, let the curve angle be π/n, and the shift distance be f/g. If n thick and n thin wedges are connected alternately, the skin surfaces are the sides of an n-gonal prism. Through a loop of wedges, the edges of length one shifted by nf/g. If nf/g is an integer, then the edges on the trapezoid sides match. Both ends of the sheet can be connected in the folded and developed states. When nf/g is a rational number, multiplying by the number of wedges creates a closed tube. When g is odd number, the wedge type should be changed for every g wedges. When g is even number, $g+1$ thick wedges and $g-1$ thin wedges are alternately connected. In both cases, $2ng$ wedges form a loop, and the sum of the shift distance is nf. The parameters in Figs. 10 and 11 satisfy these conditions. As shown in Fig. 10, $\phi_1 - \phi_2 = \pi/16$ and $t = 1/4$. As shown

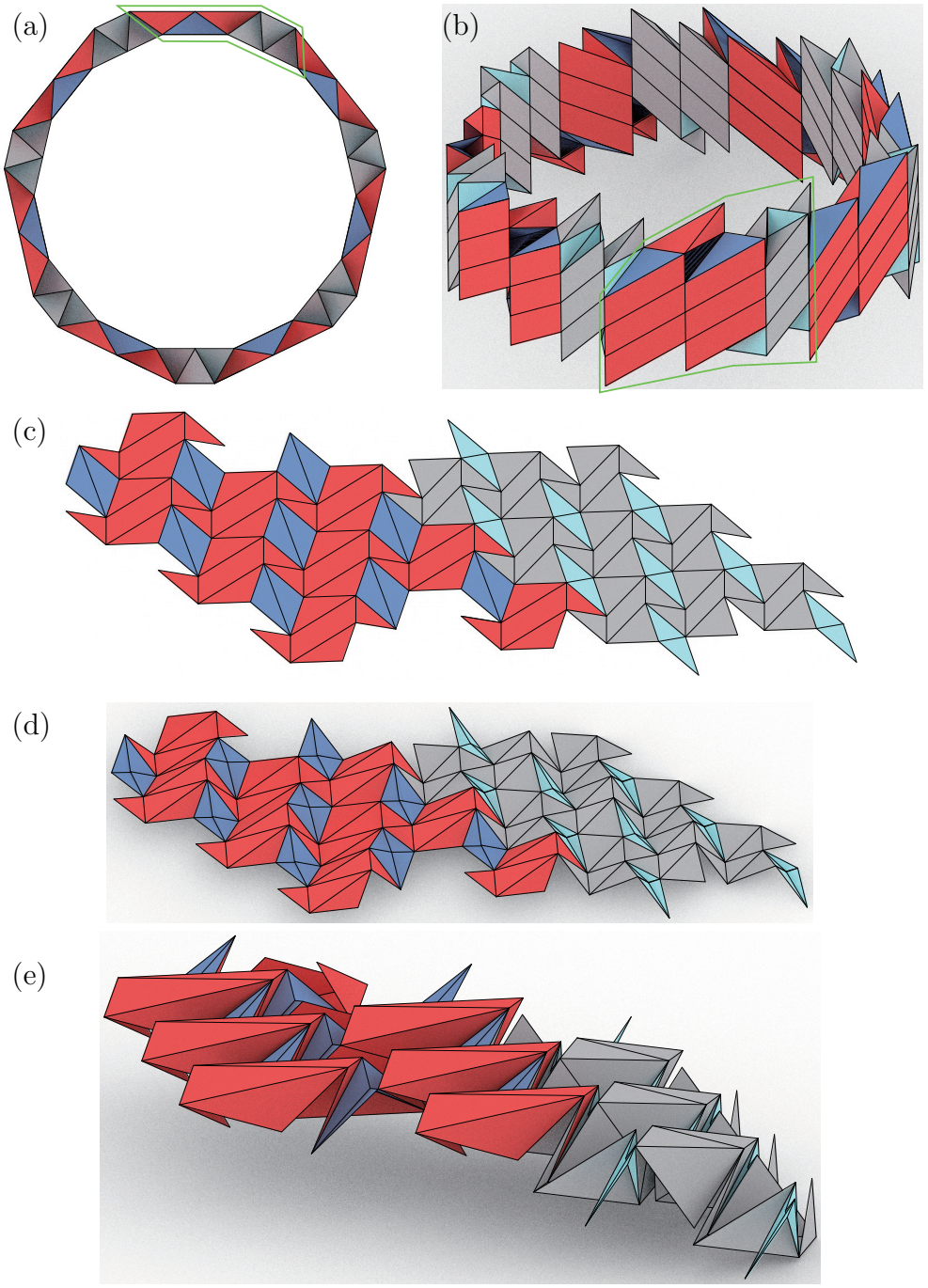

Figure 12: Cylindrical parallelogram dual tiling origami that forms nearly a tube. (a) Projection along the apex edges, (b) Oblique view, (c) Crease pattern of six wedges surrounded by the green frame in (a), (d)(e) Intermediate states of folding.

in Fig. 11, $\phi_1 - \phi_2 = \pi/72$ and $t = 1/3$. These parameters create a tubular parallelogram dual tiling origami with a valid sequence, such as "1212 . . . ".

Figure 12 shows an attempt to make a closed cylindrical parallelogram dual tiling origami that satisfies the tetrahedron conditions critically. Solving simultaneous equations (14) and (15), and $\phi_1 - \phi_2 = \pi/n$, where t is a rational, n is an integer. This is an overconstrained problem. Therefore, we attempted to obtain an approximation. When $\phi_1 \simeq 0.958378, \phi_1 - \phi_2 = \pi/7$, $t \simeq 1.4762 \simeq 31/21$; these parameters form a nearly closed tubular skin surface.

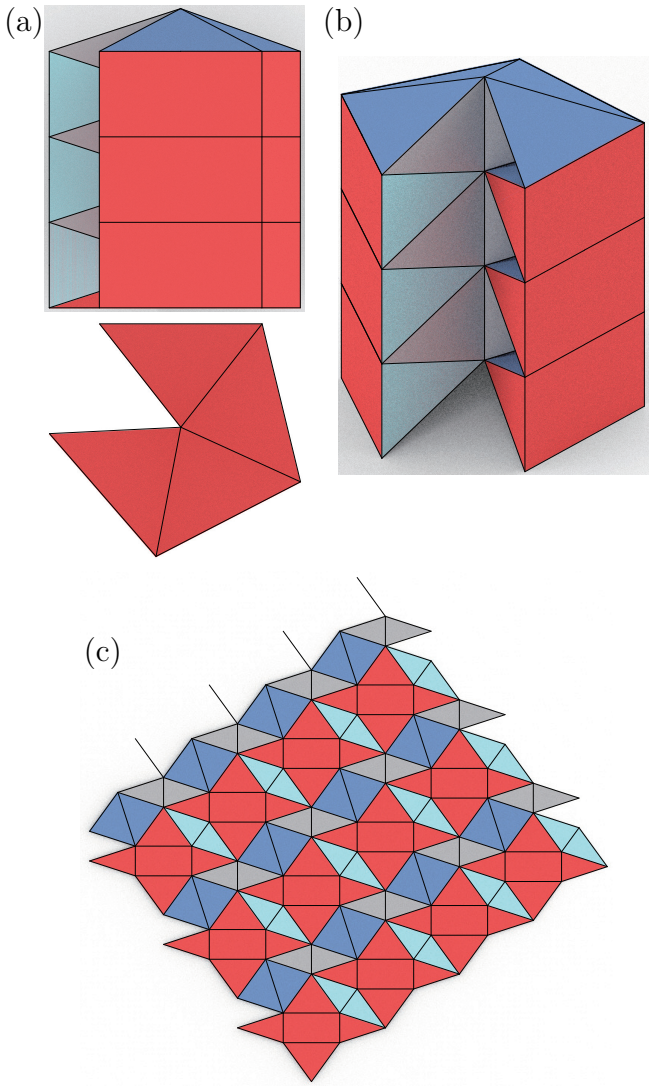

Figure 13: Cylindrical parallelogram dual tiling origami, one of the pyramids of that degenerate. The tetrahedron conditions are satisfied critically. (a) Front and top views, (b) Oblique view, (c) Crease pattern.

Figure 12 alternately connects three thick and three thin wedges. The skin surfaces are the sides of the 14-gonal prism.

4.3 Degenerate Parallelogram Dual Tiling Origami

Figure 13 shows a design with one of its pyramids having a rectangular base, i.e., $\angle DAB = \pi/2$ in its crease pattern (see Fig. 6). The base of the other partner pyramid degenerates into a line segment. In other words, B' agrees with A in Fig. 6. If we allow a degenerate pyramid to be valid, then, the pair of pyramids construct a parallelogram dual tiling origami when the tetrahedron conditions are satisfied. Degenerate parallelogram dual tiling origami can be designed by setting $t = 0$ and $\phi_i = 0$ ($i = 1$ or $i = 2$) rendering wedge i degenerate.

By symmetry, we assume that $\phi_2 = 0$. Subsequently, of the original three parameters, we have only one nominal parameter $\phi_1 \in (0, \pi/2)$. However, the design variations form a two-parameter family. This is because p is still undefined and can consider any positive value

for arbitrary ϕ_1. Therefore, we use two parameters $\phi_1 \in (0, \pi/2)$ and $p > 0$ to design the variations in the degenerate patterns. When we change p for a given ϕ_1, the shape of the isosceles triangles, which are projected pyramids along the apex edges (Fig. 13 (a)), remains similar, although their scale changes.

Figure 13 shows a special case of degenerate parallelogram dual tiling origami, where both types of tetrahedron regions are critical. Substituting $t = 0$, $\phi_2 = 0$, and $r = t/(2 \sin \phi_1 \sin \phi_2)$ into equations (14), (15), and (9), we obtain

$$\sin \phi_1 = \frac{-1 + \sqrt{5}}{2}, \tag{16}$$

$$r = \frac{1}{3 - \sqrt{5}}, \tag{17}$$

$$p = \frac{\tan 72^\circ}{2}. \tag{18}$$

$\sin \phi_1$ is the inverse of the golden ratio. The sides of Pyramid 2, which do not degenerate, have inner angles of $36^\circ, 72^\circ$, and 72°. However, $\phi_1 \simeq 38.17^\circ$ indicates that the row of wedges can not close, as shown in Fig. 13.

5 Folding Motion

The folding process of parallelogram dual tiling origami is crucial for manufacturing patterns and use in structures and cellular materials. If an origami crease pattern allows for a continuous folding motion without the deformation of each face or movement of the crease, the pattern is considered to be rigidly foldable. Therefore, the rigid foldability of parallelogram dual tiling origami is a natural and important issue.

According to our observations, parallelogram dual tiling origami, including cylindrical parallelogram dual tiling origami, is generally not rigidly foldable. To compute the folding motion and the intermediate states illustrated in Figs 4, 8, 10, 11, and 12, we used a model of folding motion where: (1) the bottom of each pyramid is diagonally folded and/or (2) the two creases in each tetrahedron region are moving during the folding motion. We observed that a diagonal split on the bottom of each pyramid is almost always necessary, whereas moving crease in each tetrahedron are sometimes not required, depending on the crease pattern of the tetrahedron region. In the future, we hope to develop a proper crease pattern that allows for rigid foldability with diagonal folding.

Cylindrical parallelogram dual tiling origami that are not rigidly foldable can be folded in practice with an actual sheet material that allows for bending. In the following section, we present examples of our design folded from sheet materials.

6 Fabrication

Cylindrical parallelogram dual tiling origami can be manufactured by the CNC plotting of creases on a sheet material and manually folding them. To demonstrate this, we fabricated a cylindrical parallelogram dual tiling origami from Fig. 11, which consists of 12 wedges (Fig. 14). We used the design system to obtain the corresponding patterns, which were then grouped into crease and boundary layers. We prepared the cutting path by converting the crease lines into dashed lines and boundary lines to solid cutting lines using *Silhouette Studio*.

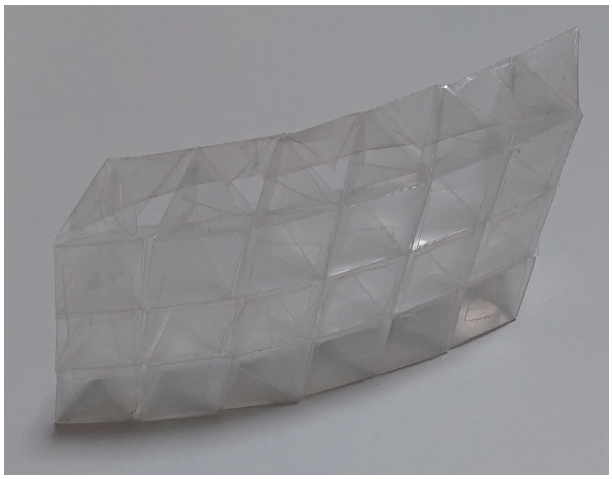

Figure 14: Parallelogram dual tiling origami shown in Fig. 11 fabricated by polypropylene sheet. We taped the skin surfaces and sides to stiffen the folded state.

We used a polypropylene sheet with a thickness of 0.2 millimeters (a file folder) and creased and cut it using a cutting plotter, *Silhouette Portrait 2*. The first author folded the patterned sheet manually. The folding was completed in approximately an hour.

It was found that the design with these chosen parameters was difficult to fold because of the bistability around the noncritical tetrahedron regions. This is seemingly because the tetrahedra are nearly critical, and only the diagonal creases fold as though they are perfectly critical. This imperfection results in the deformation of the faces in the final folded state.

In most cases, the folded state spontaneously develops. To stiffen the dual tiling origami in the final folded state, we taped the adjacent bases on the skin surfaces. In addition, the boundary edges and corners of the foldcore panel tend to be floppy; we taped the sides of the panel. The resulting foldcore taped along the wedges did not spontaneously develop.

7 Conclusion

We extended the parallelogram dual tiling origami to form globally cylindrical surfaces and named it the family of cylindrical parallelogram dual tiling origami. We demonstrated the geometric constraints of cylindrical parallelogram dual tiling origami by showing that there are two types of wedges that are compatible with each other. By aligning these two types of wedges in a particular sequence, we can create parallelogram dual tiling origami that forms various cylindrical surfaces. To design the folded shape, we introduced the three parameters ϕ_1, ϕ_2, and t, as well as showed the solution space for these parameters. We developed a design system in which users can control the curve angles, shift distance, wedge sequence. In addition, the design system has features to inversely solve these parameters to satisfy the critical conditions, allowing the crease pattern to be simple. Finally, we presented some design examples with special geometric properties, including gently curved structures and closed tubular structures.

In this study, we restricted pyramids to two-fold symmetric pyramids. Whether a more general dual tiling origami may form richer skin surfaces such as a cylindrical surface with a continuous curve angle or other developable surfaces such as conical surfaces; the question is still unanswered. Future work can include investigating the folding process using a rigid origami model and designing a dual tiling origami with rigid foldability.

Acknowledgment

This work was supported by the JSPS KAKENHIs 18H03868 and 22H04954.

References

[1] Z. R. Abel, E. D. Demaine, M. L. Demaine, H. Ito, J. Snoeyink, and R. Uehara: *Bumpy Pyramid Folding*. In *The 26th Canadian Conference on Computational-Geometry (CCCG 2014)*, 258–266. 2014.

[2] A. Adachi, T. Tachi, and Y. Yamaguchi: *Dual Tiling Origami*. J. Geom. Graph. **22**(2), 269–281, 2018.

[3] T. R. Crain: *A New Scheme to Describe Twist-Fold Tessellations*. In *Origami*^{6}, 253–264. 2014.

[4] E. D. Demaine and J. S. Ku: *Filling a Hole in a Crease Pattern: Isometric Mapping from Prescibed Boundaary Folding*. In *Origami*^{6}, 177–188. 2014.

[5] L. H. Dudte, E. Vouga, T. Tachi, and L. Mahadevan: *Programming curvature using origami tessellations*. Nat. Mater. **15**, 583–588, 2016. doi: https://doi.org/10.1038/nmat4540.

[6] S. Fujimoto and M. Nishiwaki: *Sozo suru origami asobi eno shotai (Invitation to creative origami playing)*. Asahi Culture Center 1982.

[7] Z. He and S. D. Guest: *Approximating a Target Surface with 1-DOF Rigid Origami*. In *Origami*^{7}, 505–520. 2018.

[8] Y. Hu, Y. Zhou, and H. Liang: *Constructing rigid-foldable generalized Miura-ori tessellations for curved surfaces*. ASME J. Mech. Rob. **13**(1), 2021. doi: https://doi.org/10.1115/1.4048630.

[9] Y. Klett and K. Drechsler: *Designing Technical Tessellations*. In *Origami*^{5}, 305–322. 2010.

[10] Y. Klett, M. Grzeschik, and P. Middendorf: *Comparison of Compressive Properties of Periodic Non-flat Tessellations*. In *Origami*^{6}, 371–384. 2014.

[11] R. J. Lang: *Spiderwebs, Tilings, and Flagstone Tessellations*. In *Origami*^{6}, 189–200. 2014.

[12] K. Miura: *Zeta-Core Sandwich – Its Concept and Realization*. Institute of Space and Aeronautical Science, University of Tokyo **37**(6), 137–164, 1972.

[13] K. Miura: *New Structural Form of Sandwich Core*. J. Aircr. **12**, 437–441, 1975. doi: https://doi.org/10.2514/3.44468.

[14] K. Miura: *The science of Miura-ori: A review*. In R. J. Lang, ed., *Origami*^{4}*: Fourth International Meeting of Origami science, mathematics, and education*, 87–100. 2009.

[15] R. D. Resch and H. Christiansen: *The Design and Analysis of Kinematic Folded Plate Systems*. Proceedings of IASS Symposium on Folded Plates and Prismatic Structures 1970.

[16] K. Saito, T. Nojima, and I. Hagiwara: *Relation between Geometrical Patterns and Mechanical Properties in Newly Developed Light-Weight Core Panels*. Trans. Japan Soc. Mech. Eng. Ser. A **74**(748), 1580–1586, 2008. doi: 10.1299/kikaia.74.1580.

[17] K. Suto, A. Adachi, T. Tachi, and Y. Yamaguchi: *An Edge-Extrusion Approach to Generate Extruded Miura-Ori and Its Double Tiling Origami Patterns*. In *Origami*^{7}, 435–450. 2018.

[18] T. Tachi: *Origamizing Polyhedral Surfaces*. IEEE Trans. Vis. Comput. Graph. **16**(2), 298–311, 2010. doi: 10.1109/TVCG.2009.67.

[19] T. Tachi: *Designing Freeform Origami Tessellations by Generalizing Resch's Patterns*. ASME J. Mech. Des. **135**(11), 2013. doi: 10.1115/1.4025389.

[20] Z. Xiang, Z. Shixi, W. Hai, and Y. Zhong: *Geometric design and mechanical properties of cylindrical foldcore sandwich structures*. Thin Wall. Struct. **89**, 116–130, 2015. doi: 10.1016/j.tws.2014.12.017.

[21] Y. Yoshimura: *On the mechanism of buckling of a circular cylindrical shell under axial compression*. Technical Memorandum 1390, National Advisory Committee for Aeronautics, 1955.

Internet Sources

[22] R. J. Lang: *Octet Truss, opus 652*, 2014. https://langorigami.com/artwork/octet-truss-opus-652/. Accessed on October 30, 2020.

Received May 26, 2022; final form October 2, 2022.